

ISU-HET-99-10
August 1999

Hyperon Nonleptonic Decays in Chiral Perturbation Theory Reexamined

A. Abd El-Hady^(a,b) and Jusak Tandean^(c)

(a) Physics Department, Zagazig University, Zagazig, Egypt

*(b) International Institute of Theoretical and Applied Physics,
Iowa State University, Ames, IA 50011*

(c) Department of Physics and Astronomy, Iowa State University, Ames, IA 50011

Abstract

We recalculate the leading nonanalytic contributions to the amplitudes for hyperon nonleptonic decays in chiral perturbation theory. Our results partially disagree with those calculated before, and include new terms previously omitted in the P-wave amplitudes. Although these modifications are numerically significant, they do not change the well-known fact that good agreement with experiment cannot be simultaneously achieved using one-loop S- and P-wave amplitudes.

1 Introduction

A number of papers have been devoted to the study of hyperon nonleptonic decays of the form $B \rightarrow B'\pi$ within the framework of chiral perturbation theory (χ PT). These papers have dealt with both the $|\Delta\mathbf{I}| = 1/2$ components [1, 2, 3, 4, 5, 6] and the $|\Delta\mathbf{I}| = 3/2$ components [7, 8] of the decay amplitudes. Calculations of the dominant $|\Delta\mathbf{I}| = 1/2$ amplitudes have led to mixed results. Specifically, theory can give a good description of either the S-waves or the P-waves, but not both simultaneously.

In this paper, we revisit the calculation of the leading nonanalytic contributions to the $|\Delta\mathbf{I}| = 1/2$ amplitudes. Our results disagree for some of the decay diagrams with those of Ref. [2], which is the most recent published work with the same approach. Furthermore, our results include new terms in the P-waves that were previously omitted. We will show that, even though these modifications are numerically important, they do not affect the main conclusions of Ref. [2].

In Section 2 we review the basic chiral Lagrangian used for our calculation in the heavy-baryon formalism. Section 3 contains detailed results of our calculation of the leading nonanalytic corrections. Finally, in Section 4 we compare our results with experiment and present some discussions.

2 Chiral Lagrangian

The chiral Lagrangian that describes the interactions of the lowest-lying mesons and baryons is written down in terms of the lightest meson-octet, baryon-octet, and baryon-decuplet fields [1, 3, 9]. The meson and baryon octets are collected into 3×3 matrices ϕ and B , respectively, and the decuplet fields are represented by the Rarita-Schwinger tensor T_{abc}^μ , where the notation here follows that of Ref. [8]. The octet bosons enter through the exponential $\Sigma = \exp(i\phi/f)$, where f is the pion-decay constant in the chiral-symmetry limit. In the heavy-baryon formalism [3, 10], the chiral Lagrangian is rewritten in terms of velocity-dependent baryon fields, $B_v(x) = e^{im_B \gamma^\mu v \cdot x} B(x)$ and $T_v^\mu(x) = e^{im_B \gamma^\mu v \cdot x} T^\mu(x)$, where m_B is the baryon-octet mass in the chiral-symmetry limit.

For the strong interactions, the leading-order chiral Lagrangian is given by [3, 10, 11]

$$\begin{aligned} \mathcal{L}^s = & \frac{1}{4}f^2 \text{Tr}(\partial^\mu \Sigma^\dagger \partial_\mu \Sigma) + \text{Tr}(\bar{B}_v i v \cdot \mathcal{D} B_v) + 2D \text{Tr}(\bar{B}_v S_v^\mu \{ \mathcal{A}_\mu, B_v \}) + 2F \text{Tr}(\bar{B}_v S_v^\mu [\mathcal{A}_\mu, B_v]) \\ & - \bar{T}_v^\mu i v \cdot \mathcal{D} T_{v\mu} + \Delta m \bar{T}_v^\mu T_{v\mu} + \mathcal{C}(\bar{T}_v^\mu \mathcal{A}_\mu B_v + \bar{B}_v \mathcal{A}_\mu T_v^\mu) + 2\mathcal{H} \bar{T}_v^\mu S_v \cdot \mathcal{A} T_{v\mu}, \end{aligned} \quad (1)$$

where Δm denotes the mass difference between the decuplet and octet baryons in the chiral-symmetry limit, S_v^μ is a velocity-dependent spin operator, and additional details can be found in Ref. [8]. Explicit breaking of chiral symmetry, to leading order in the mass of the strange quark

and in the limit $m_u = m_d = 0$, is introduced via the Lagrangian [12]

$$\begin{aligned} \mathcal{L}_{m_q}^s &= a \operatorname{Tr}(M\Sigma^\dagger + \Sigma M^\dagger) + b_D \operatorname{Tr}(\bar{B}_v \{ \xi^\dagger M \xi^\dagger + \xi M^\dagger \xi, B_v \}) + b_F \operatorname{Tr}(\bar{B}_v [\xi^\dagger M \xi^\dagger + \xi M^\dagger \xi, B_v]) \\ &\quad + \sigma \operatorname{Tr}(M\Sigma^\dagger + \Sigma M^\dagger) \operatorname{Tr}(\bar{B}_v B_v) \\ &\quad + c \bar{T}_v^\mu (\xi^\dagger M \xi^\dagger + \xi M^\dagger \xi) T_{v\mu} - \tilde{\sigma} \operatorname{Tr}(M\Sigma^\dagger + \Sigma M^\dagger) \bar{T}_v^\mu T_{v\mu}, \end{aligned} \quad (2)$$

where $M = \operatorname{diag}(0, 0, m_s)$. In this limit, the pion is massless and the η_8 mass is related to the kaon mass by $m_{\eta_8}^2 = \frac{4}{3} m_K^2$. Moreover, mass splittings within the baryon octet and decuplet occur to linear order in m_s .

As is well known, the weak interactions that generate hyperon nonleptonic decays are described by a $|\Delta S| = 1$ Hamiltonian that transforms as $(8_L, 1_R) \oplus (27_L, 1_R)$ under $SU(3)_L \times SU(3)_R$ rotations. Experimentally, the octet piece dominates the 27-plet piece, as indicated by the fact that the $|\Delta \mathbf{I}| = 1/2$ components of the decay amplitudes are larger than the $|\Delta \mathbf{I}| = 3/2$ components by about twenty times [8, 13]. We shall, therefore, assume in what follows that the decays are completely characterized by the $(8_L, 1_R)$, $|\Delta \mathbf{I}| = 1/2$ interactions. The leading-order chiral Lagrangian for such interactions is [1, 2]

$$\begin{aligned} \mathcal{L}^w &= h_D \operatorname{Tr}(\bar{B}_v \{ \xi^\dagger h \xi, B_v \}) + h_F \operatorname{Tr}(\bar{B}_v [\xi^\dagger h \xi, B_v]) + h_C \bar{T}_v^\mu \xi^\dagger h \xi T_{v\mu} \\ &\quad + \gamma_8 f^2 \operatorname{Tr}(h \partial_\mu \Sigma \partial^\mu \Sigma^\dagger) + \text{h.c.}, \end{aligned} \quad (3)$$

where h is a 3×3 matrix with elements $h_{ij} = \delta_{i2} \delta_{3j}$, the parameters $h_{D,F,C}$ will be determined below, and $\gamma_8 \approx 8.0 \times 10^{-8}$ as extracted from kaon decays.

3 Amplitudes

Using the heavy-baryon approach, we express the amplitude for the decay $B \rightarrow B' \pi$ in the form

$$i\mathcal{M}_{B \rightarrow B' \pi} = G_F m_{\pi^+}^2 \bar{u}_{B'} (\mathcal{A}_{BB' \pi}^{(S)} + 2k \cdot S_v \mathcal{A}_{BB' \pi}^{(P)}) u_B, \quad (4)$$

where the superscripts refer to the S- and P-wave contributions and k is the outgoing four-momentum of the pion. The $|\Delta \mathbf{I}| = 1/2$ amplitudes satisfy the isospin relations

$$\begin{aligned} \mathcal{M}_{\Sigma^+ \rightarrow n \pi^+} - \sqrt{2} \mathcal{M}_{\Sigma^+ \rightarrow p \pi^0} - \mathcal{M}_{\Sigma^- \rightarrow n \pi^-} &= 0, \\ \sqrt{2} \mathcal{M}_{\Lambda \rightarrow n \pi^0} + \mathcal{M}_{\Lambda \rightarrow p \pi^-} &= 0, \quad \sqrt{2} \mathcal{M}_{\Xi^- \rightarrow \Lambda \pi^0} + \mathcal{M}_{\Xi^- \rightarrow \Lambda \pi^-} = 0, \end{aligned} \quad (5)$$

and so only four of them are independent. Following Refs. [1, 2], we choose the four to be $\Sigma^+ \rightarrow n \pi^+$, $\Sigma^- \rightarrow n \pi^-$, $\Lambda \rightarrow p \pi^-$ and $\Xi^- \rightarrow \Lambda \pi^-$.

In calculating the decay amplitudes, we will consider the leading-order terms and their one-loop corrections. For the loop diagrams, we will adopt the approach taken in Ref. [2] by keeping

only calculable terms of $\mathcal{O}(m_s \ln m_s)$ and $\mathcal{O}(m_s^2 \ln m_s)$. The latter, $\mathcal{O}(m_s^2 \ln m_s)$, terms are formally smaller than the former, but are included because, as was argued in Ref. [2], they arise from graphs proportional to γ_8 in Eq. 3, whose value is enhanced with respect to naive expectation, thereby generating contributions comparable to the $\mathcal{O}(m_s \ln m_s)$ terms, which are proportional to $h_{D,F,C}$. At the one-loop level, there are also corrections of $\mathcal{O}(m_s)$, but these are not computable due to the many counterterms that contribute at the same order. To take into account the error associated with neglecting all these terms,¹ we will incorporate some theoretical uncertainties when comparing theory with experiment. It is possible to perform a complete one-loop calculation including all counterterms, but then one loses predictive power as there are more free parameters than data.²

We write the S- and P-wave decay amplitudes at the one-loop level in the form

$$\begin{aligned}\mathcal{A}_{BB'\pi}^{(S)} &= \frac{1}{\sqrt{2}f_\pi} \left[\alpha_{BB'}^{(S)} + \left(\bar{\beta}_{BB'}^{(S)} - \bar{\lambda}_{BB'\pi} \alpha_{BB'}^{(S)} \right) \frac{m_K^2}{16\pi^2 f_P^2} \ln \frac{m_K^2}{\mu^2} \right], \\ \mathcal{A}_{BB'\pi}^{(P)} &= \frac{1}{\sqrt{2}f_\pi} \left[\alpha_{BB'}^{(P)} + \left(\bar{\beta}_{BB'}^{(P)} - \bar{\lambda}_{BB'\pi} \alpha_{BB'}^{(P)} \right) \frac{m_K^2}{16\pi^2 f_P^2} \ln \frac{m_K^2}{\mu^2} + \tilde{\alpha}_{BB'}^{(P)} \right],\end{aligned}\quad (6)$$

where $f_\pi \approx 92.4$ MeV is the physical pion-decay constant and $f_P = f_\pi$ or $f_K (\approx 1.22 f_\pi)$. Contributions from tree-level and one-loop diagrams, shown in Figures 1, 2, and 3, are represented by $\alpha_{BB'}$ and $\bar{\beta}_{BB'} = \beta_{BB'} + \beta'_{BB'}$, respectively, where $\beta_{BB'}$ comes from one-loop decay graphs involving only octet baryons and $\beta'_{BB'}$ arises from those with internal decuplet-baryon lines. The coefficient $\bar{\lambda}_{BB'\pi}$ contains contributions from baryon and pion wave-function renormalization as well as the renormalization of the pion-decay constant. The P-wave term $\tilde{\alpha}_{BB'}^{(P)}$ results from one-loop corrections to the propagator in the lowest-order P-wave diagrams in Figure 1(b). The expressions for $\alpha_{BB'}$, $\beta_{BB'}$, $\beta'_{BB'}$, $\bar{\lambda}_{BB'\pi}$, and $\tilde{\alpha}_{BB'}^{(P)}$ are given in the Appendix.



Figure 1: Tree-level diagrams for (a) S-wave and (b) P-wave hyperon nonleptonic decays. In all figures, a solid (dashed) line denotes a baryon-octet (meson-octet) field, and a solid dot (hollow square) represents a strong (weak) vertex, with the strong vertices being generated by \mathcal{L}^s in Eq. (1). Here the weak vertices come from the $h_{D,F}$ terms in Eq. (3).

We would now like to point out where our theoretical results differ from those of Ref. [2]. Firstly, starting from the same decay diagrams (Figures 1, 2, and 3) as those used therein, we found the

¹To simplify our calculation and to follow Ref. [2], we have also neglected $\mathcal{O}(m_s)$ terms which are calculable from the heavy-baryon expansion of the relativistic Lagrangian [14], as well as calculable $\mathcal{O}(m_s^{3/2})$ contributions (from the one-loop diagrams) that we expect to be small.

²Such a calculation was done in Ref. [6].

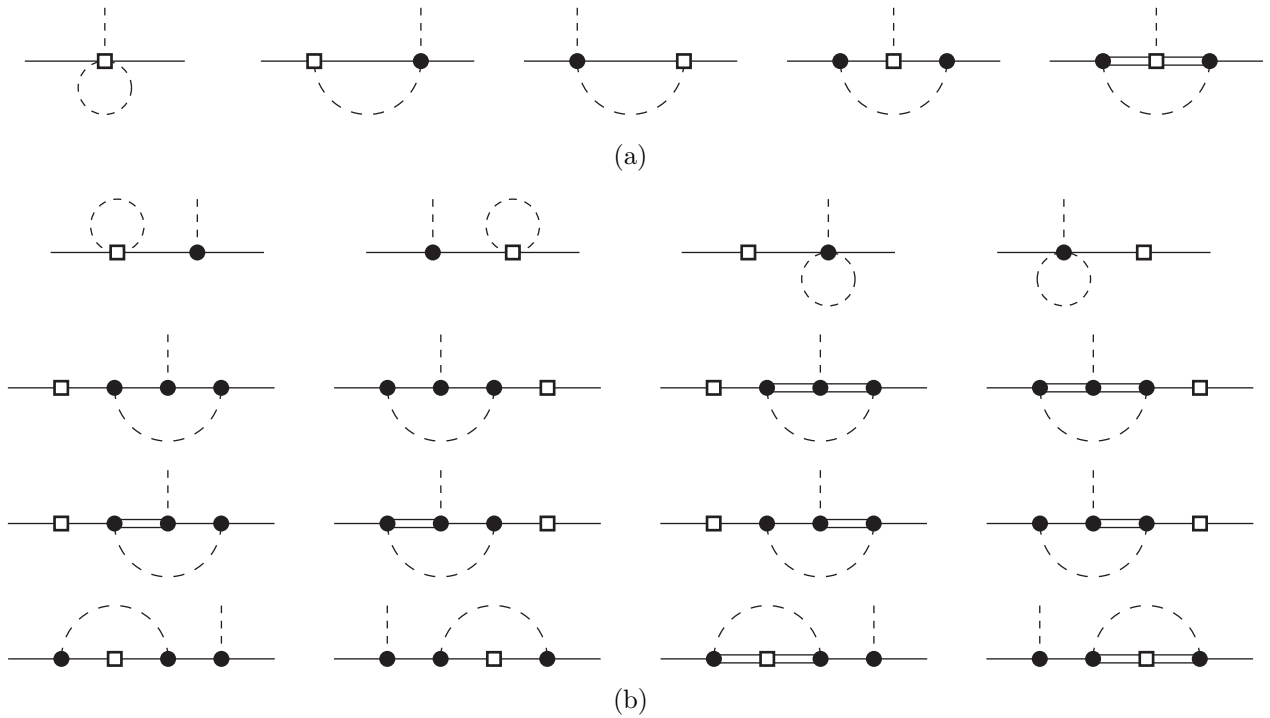


Figure 2: One-loop diagrams contributing to (a) S-wave and (b) P-wave hyperon nonleptonic decay amplitudes, with weak vertices from the $h_{D,F,C}$ terms in Eq. (3). The double lines represent baryon-decuplet fields.

same expressions for $\alpha_{BB'}^{(S,P)}$, $\bar{\beta}_{BB'}^{(S,P)}$, and $\bar{\lambda}_{BB'\pi}$, with the exception of terms in $\bar{\beta}_{BB'}^{(S,P)}$ proportional to γ_8 , corresponding to the graphs in Figure 3. Amongst these γ_8 terms, we were able to reproduce only the expression for $\bar{\beta}_{\Sigma^+ n}^{(S)}$ in Ref. [2]. Secondly, we have included in the P-wave amplitudes the terms $\tilde{\alpha}_{BB'}^{(P)}$, which were missing in Ref. [2] (and in Ref. [1]) and were partially addressed in Ref. [5].³ In the next section, we will discuss how these theoretical modifications affect the prediction for the amplitudes.

4 Numerical Results and Discussion

From the measurement of the decay rate and the decay-distribution asymmetry parameter α , it is possible to extract the value of the S- and P-wave amplitudes for each hyperon decay [13]. Using the most recent data [15], we find the results presented in Table 1,⁴ where s, p are related to $\mathcal{A}_{BB'\pi}^{(S,P)}$ by $s = \mathcal{A}^{(S)}$ and $p = -|\mathbf{k}|\mathcal{A}^{(P)}$, with \mathbf{k} being the pion three-momentum in the rest frame of the decaying baryon. These numbers are nearly identical to those quoted in Ref. [2].

³These corrections were considered for the $|\Delta \mathbf{I}| = 3/2$ case in Ref. [8].

⁴In extracting these numbers, final-state interactions have been ignored and experimental masses used.

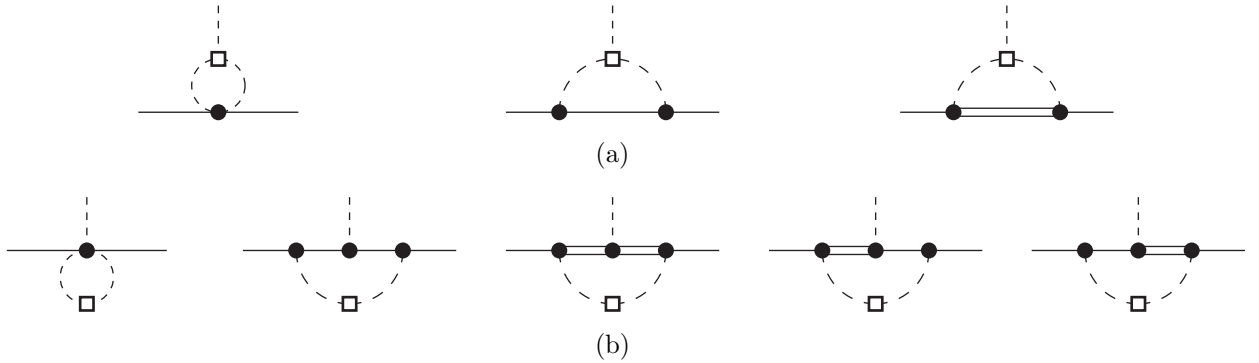


Figure 3: One-loop diagrams contributing to (a) S-wave and (b) P-wave hyperon nonleptonic decay amplitudes, with weak vertices from the γ_8 term in Eq. (3).

Table 1: Experimental values for S- and P-wave amplitudes.

Decay mode	<i>s</i>	<i>p</i>
$\Sigma^+ \rightarrow n\pi^+$	0.06 ± 0.01	1.81 ± 0.01
$\Sigma^+ \rightarrow p\pi^0$	-1.43 ± 0.05	1.17 ± 0.06
$\Sigma^- \rightarrow n\pi^-$	1.88 ± 0.01	-0.06 ± 0.01
$\Lambda \rightarrow p\pi^-$	1.42 ± 0.01	0.52 ± 0.01
$\Lambda \rightarrow n\pi^0$	-1.04 ± 0.02	-0.39 ± 0.03
$\Xi^- \rightarrow \Lambda\pi^-$	-1.98 ± 0.01	0.48 ± 0.02
$\Xi^0 \rightarrow \Lambda\pi^0$	1.51 ± 0.02	-0.32 ± 0.02

To evaluate how our results describe the data, we employ the parameter values used in Ref. [2]: $D = 0.61$, $F = 0.40$, $\mathcal{C} = 1.6$, $\mathcal{H} = -1.9$, $f_P = f_\pi$, and $\mu = 1$ GeV. We also need the values of the parameters that appear in Eq. (2), as they are contained in $\tilde{\alpha}_{BB'}^{(P)}$. Following Ref. [8], we choose

$$b_D m_s = \frac{3}{8} (m_\Sigma - m_\Lambda) \approx 0.0290 \text{ GeV} , \quad b_F m_s = \frac{1}{4} (m_N - m_\Xi) \approx -0.0948 \text{ GeV} , \quad (7)$$

$$c m_s = \frac{1}{2} (m_\Omega - m_\Delta) \approx 0.220 \text{ GeV} , \quad \Delta m - 2 (\tilde{\sigma} - \sigma) m_s = m_\Delta - m_\Sigma \approx 0.0389 \text{ GeV} ,$$

where the fourth parameter is the only combination of Δm , σm_s and $\tilde{\sigma} m_s$ which occurs in $\tilde{\alpha}_{BB'}^{(P)}$.

The values of h_D , h_F , and h_C in Eq. 3 are determined by a least-squares fit using the four S-wave amplitudes that are not related by isospin. Fitting the one-loop formulas to experiment thus yields $h_D = -0.84 \pm 0.34$, $h_F = 0.78 \pm 0.68$, and $h_C = 4.16 \pm 7.63$, where all of these parameters are written in units of $\sqrt{2} f_\pi G_F m_{\pi^+}^2$. The quoted errors reflect an estimate of the theoretical uncertainty due to the terms neglected in our calculation. To compute them, we followed Ref. [2] by adding a canonical error of 0.30 to each S-wave amplitude and ignoring the much smaller experimental error.⁵ The uncertainty in h_C is large because it enters the amplitudes only at loop level and so

⁵This is consistent with the fact that most of the neglected contributions are of $\mathcal{O}(m_s)$, which amount to corrections of about $m_s/\Lambda \sim 20\%$, with $\Lambda \sim 1$ GeV being the chiral-symmetry breaking scale.

it is poorly constrained. The numbers we found above are different from those found in Ref. [2]: $h_D = -0.35 \pm 0.09$, $h_F = 0.86 \pm 0.05$, and $h_C = -0.36 \pm 0.65$. The discrepancy in the central values of these two sets of numbers indicates that the theoretical modifications we made are numerically important, but the large errors in the parameters, especially those in h_C and h_F , make it appear less so. For comparison, fitting the tree-level amplitudes gives $h_D = -0.55 \pm 0.29$ and $h_F = 1.37 \pm 0.17$. It is worth mentioning that, despite their variations, these three sets of numbers are still consistent with their expected values according to naive dimensional analysis [18].

Using the parameter values from our fit above, we obtained the numerical results presented in Table 2. Since the S-wave formula for $\Sigma^+ \rightarrow n\pi^+$ does not depend on $h_{D,F,C}$, the three-parameter fit leads to exact agreement with experiment for the other three S-wave channels. As a consequence, the Lee-Sugawara relation [16], $3s_{\Sigma^- \rightarrow n\pi^-}/\sqrt{6} + s_{\Lambda \rightarrow p\pi^-} + 2s_{\Xi^- \rightarrow \Lambda\pi^-} = 0$, which is a prediction of SU(3) symmetry and agrees well with data, is well satisfied. A good fit (using all of the seven S-waves) was also obtained in Ref. [2], but the individual tree and loop contributions therein are numerically different from ours, in some cases markedly, albeit within expectations. As in Ref. [2], we can see in Table 2 that some of the loop corrections in the S-waves are comparable in size to the lowest-order results even though they are naively expected to be smaller by about a factor of 20%. In addition, we found that $\mathcal{O}(m_s^2 \ln m_s)$ contributions (from diagrams proportional to γ_8) are sometimes larger than those of $\mathcal{O}(m_s \ln m_s)$. This lack of convergence is an inherent flaw in a perturbative calculation where the expansion parameter, m_s/Λ , is not sufficiently small and there are many loop-diagrams involved. The problem also occurs in the $|\Delta I| = 3/2$ sector [8] and in other cases [17]. For the P-waves, the disagreement between theory and experiment is worse than before. The tree-level contributions remain suppressed with respect to the chiral-logarithmic corrections because of the near cancellations of the two terms in the tree-level formulas [2], and the loop correction receives a sizable contribution from the new term $\tilde{\alpha}_{BB'}^{(P)}$.

Table 2: Experimental and theoretical values of S- and P-wave amplitudes for $h_D = -0.84$, $h_F = 0.78$, and $h_C = 4.16$.

Decay mode	s_{expt}	s_{theory}	s_{tree}	s_{loop}	$s_{\text{loop}}^{(\text{oct})}$	$s_{\text{loop}}^{(\text{dec})}$
$\Sigma^+ \rightarrow n\pi^+$	0.06	-0.09	0.00	-0.09	0.13	-0.22
$\Sigma^- \rightarrow n\pi^-$	1.88	1.88	1.62	0.26	0.40	-0.14
$\Lambda \rightarrow p\pi^-$	1.42	1.42	0.61	0.81	0.24	0.58
$\Xi^- \rightarrow \Lambda\pi^-$	-1.98	-1.98	-1.29	-0.69	-0.22	-0.46
Decay mode	p_{expt}	p_{theory}	p_{tree}	p_{loop}	$p_{\text{loop}}^{(\text{oct})}$	$p_{\text{loop}}^{(\text{dec})}$
$\Sigma^+ \rightarrow n\pi^+$	1.81	2.41	-0.40	2.81	0.07	2.74
$\Sigma^- \rightarrow n\pi^-$	-0.06	1.93	-0.16	2.10	0.08	2.01
$\Lambda \rightarrow p\pi^-$	0.52	-1.13	-0.03	-1.10	-0.09	-1.01
$\Xi^- \rightarrow \Lambda\pi^-$	0.48	2.17	-0.22	2.39	0.06	2.33

The dependence of the one-loop contributions in Eq. (6) on the renormalization scale μ is canceled by the μ -dependence of the counterterms that have been neglected, and so our one-loop amplitudes depend on the choice of μ . It is, therefore, important to know how our results change as μ varies. At the same time, we would also like to know how our results will differ if we make the following two changes in order to reduce, at least at one-loop order, the effects of kaon and eta loops, which may be overestimated in χ PT [19]. We will set $f_P = f_K \approx 113$ MeV, instead of f_π , in the amplitudes in Eq. (6), for the difference will appear at higher orders. Also, we will use the same values of D , F , and \mathcal{H} as before, but now $\mathcal{C} = 1.2$, all of which are the favored values from one-loop fits to semileptonic and strong hyperon decays [11, 20]. We will consider three different values of μ , and, for each of them, perform a least-squares fit as before to determine the values of $h_{D,F,C}$. The results of these fits, along with the corresponding predictions for the amplitudes, are given in Table 3.

Table 3: Experimental and theoretical values of S- and P-wave amplitudes for various values of μ , and the corresponding values of h_D , h_F , and h_C .

$\mu = 0.8$ GeV, $h_D = -0.76 \pm 0.37$, $h_F = 0.89 \pm 0.74$, $h_C = 8.6 \pm 20.4$								
Decay mode	s_{expt}	s_{theory}	s_{tree}	s_{loop}	p_{expt}	p_{theory}	p_{tree}	p_{loop}
$\Sigma^+ \rightarrow n\pi^+$	0.06	0.00	0.00	0.00	1.81	0.76	-0.33	1.09
$\Sigma^- \rightarrow n\pi^-$	1.88	1.88	1.65	0.23	-0.06	0.69	-0.08	0.77
$\Lambda \rightarrow p\pi^-$	1.42	1.42	0.78	0.64	0.52	-0.55	-0.12	-0.43
$\Xi^- \rightarrow \Lambda\pi^-$	-1.98	-1.98	-1.40	-0.58	0.48	1.06	-0.13	1.19
$\mu = 1$ GeV, $h_D = -0.78 \pm 0.33$, $h_F = 0.82 \pm 0.68$, $h_C = 7.2 \pm 14.7$								
Decay mode	s_{expt}	s_{theory}	s_{tree}	s_{loop}	p_{expt}	p_{theory}	p_{tree}	p_{loop}
$\Sigma^+ \rightarrow n\pi^+$	0.06	0.00	0.00	0.00	1.81	0.82	-0.36	1.17
$\Sigma^- \rightarrow n\pi^-$	1.88	1.88	1.60	0.28	-0.06	0.80	-0.12	0.91
$\Lambda \rightarrow p\pi^-$	1.42	1.42	0.68	0.74	0.52	-0.65	-0.08	-0.58
$\Xi^- \rightarrow \Lambda\pi^-$	-1.98	-1.98	-1.32	-0.66	0.48	1.21	-0.17	1.38
$\mu = 1.2$ GeV, $h_D = -0.80 \pm 0.30$, $h_F = 0.77 \pm 0.64$, $h_C = 6.7 \pm 12.1$								
Decay mode	s_{expt}	s_{theory}	s_{tree}	s_{loop}	p_{expt}	p_{theory}	p_{tree}	p_{loop}
$\Sigma^+ \rightarrow n\pi^+$	0.06	0.00	0.00	0.00	1.81	0.86	-0.38	1.24
$\Sigma^- \rightarrow n\pi^-$	1.88	1.88	1.57	0.31	-0.06	0.88	-0.14	1.02
$\Lambda \rightarrow p\pi^-$	1.42	1.42	0.62	0.80	0.52	-0.72	-0.05	-0.68
$\Xi^- \rightarrow \Lambda\pi^-$	-1.98	-1.98	-1.27	-0.71	0.48	1.34	-0.20	1.53

We can see that the central values of $h_{D,F}$ are relatively stable with respect to changes in the other parameters, and h_C is less so, but the different values of these weak parameters are still consistent with each other in view of their large errors. The tree and loop terms of the S-waves are also relatively stable against the parameter changes. The loop terms of the P-waves, however, change significantly as we move from Table 2 to Table 3, whereas the P-waves in Table 3 do not as μ is varied. This significant change is mainly due to our choice of $f_P = f_K$ and $\mathcal{C} = 1.2$ for Table 3,

which leads to a dramatic decrease of the loop contributions with respect to the leading-order terms, alleviating the discrepancy between theory and experiment. Comparison of the $\mu = 1$ GeV cases in the two tables shows that this choice also leads to a slight reduction in the lack of chiral convergence in our S-wave formulas. Finally, we should mention that our one-loop formulas, with the sets of parameter values used in Table 3, can describe both the (seven) S- and P-wave data better than either a tree-level fit or the one-loop fit of Ref. [2] can, although the P-waves remain poorly reproduced.

In conclusion, we have reexamined the one-loop analysis of the amplitudes for hyperon nonleptonic decays in chiral perturbation theory, concentrating on the leading nonanalytic contributions to the amplitudes. We have discussed how our theoretical results differed from those previously calculated using the same approach. Even though the differences are numerically important, they do not alter the well-known fact that a good prediction at one-loop level cannot simultaneously be made for the S- and P-wave amplitudes. Nevertheless, our results suggest that a judicious choice of the parameter values in the theory can, at least at one-loop level, lead to a sizable reduction of the large kaon-loop effects relative to the lowest-order contributions and yield an improved fit to experiment.

Acknowledgments We would like to thank G. Valencia for many helpful discussions and suggestions. J. T. thanks the Fermilab Theory Group for hospitality during its Summer Visitors Program while part of this work was done. This work was supported in part by DOE under contract number DE-FG02-92ER40730. The work of A. A. was supported in part by DOE under contract number DE-FG02-87ER40371, and by the International Institute of Theoretical and Applied Physics, Iowa State University, Ames, Iowa.

Appendix

From the tree-level diagrams displayed in Figure 1,

$$\begin{aligned}
\alpha_{\Sigma^+ n}^{(S)} &= 0, & \alpha_{\Sigma^- n}^{(S)} &= -h_D + h_F, & \alpha_{\Lambda p}^{(S)} &= \frac{1}{\sqrt{6}}(h_D + 3h_F), & \alpha_{\Xi^- \Lambda}^{(S)} &= \frac{1}{\sqrt{6}}(h_D - 3h_F), \\
\alpha_{\Sigma^+ n}^{(P)} &= \frac{-D(h_D - h_F)}{m_\Sigma - m_N} - \frac{\frac{1}{3}D(h_D + 3h_F)}{m_\Lambda - m_N}, \\
\alpha_{\Sigma^- n}^{(P)} &= \frac{-F(h_D - h_F)}{m_\Sigma - m_N} - \frac{\frac{1}{3}D(h_D + 3h_F)}{m_\Lambda - m_N}, \\
\alpha_{\Lambda p}^{(P)} &= \frac{2D(h_D - h_F)}{\sqrt{6}(m_\Sigma - m_N)} + \frac{(D + F)(h_D + 3h_F)}{\sqrt{6}(m_\Lambda - m_N)}, \\
\alpha_{\Xi^- \Lambda}^{(P)} &= \frac{-2D(h_D + h_F)}{\sqrt{6}(m_\Xi - m_\Sigma)} - \frac{(D - F)(h_D - 3h_F)}{\sqrt{6}(m_\Xi - m_\Lambda)}.
\end{aligned}$$

From one-loop diagrams involving only octet baryons, shown in Figures 2 and 3,

$$\begin{aligned}
\beta_{\Sigma^+ n}^{(S)} &= -2D^2(m_\Sigma - m_N)\gamma_8, \\
\beta_{\Sigma^- n}^{(S)} &= \frac{11}{12}(h_D - h_F) + \left(\frac{7}{6}D^2 - 3DF - \frac{3}{2}F^2\right)h_D + \left(\frac{5}{6}D^2 + 5DF + \frac{3}{2}F^2\right)h_F \\
&\quad + \left[\left(\frac{7}{6} + 4D^2 - 9DF + 3F^2\right)(m_\Sigma - m_N) + (D^2 + 3DF)(m_\Lambda - m_N)\right]\gamma_8, \\
\beta_{\Lambda p}^{(S)} &= \frac{1}{\sqrt{6}}\left[-\frac{11}{12}(h_D + 3h_F) + \left(\frac{19}{6}D^2 - 11DF + \frac{9}{2}F^2\right)h_D + \left(\frac{7}{2}D^2 - 15DF + \frac{27}{2}F^2\right)h_F\right] \\
&\quad + \frac{1}{\sqrt{6}}\left[\left(\frac{7}{2} + 2D^2 - 3DF + 9F^2\right)(m_\Lambda - m_N) + (-9D^2 + 9DF)(m_\Sigma - m_N)\right]\gamma_8, \\
\beta_{\Xi^- \Lambda}^{(S)} &= \frac{1}{\sqrt{6}}\left[-\frac{11}{12}(h_D - 3h_F) + \left(\frac{19}{6}D^2 + 11DF + \frac{9}{2}F^2\right)h_D - \left(\frac{7}{2}D^2 + 15DF + \frac{27}{2}F^2\right)h_F\right] \\
&\quad + \frac{1}{\sqrt{6}}\left[\left(-\frac{7}{2} + 7D^2 + 6DF - 9F^2\right)(m_\Xi - m_\Lambda) + (-9D^2 - 9DF)(m_\Sigma - m_\Lambda)\right]\gamma_8, \\
\beta_{\Sigma^+ n}^{(P)} &= \frac{\frac{17}{12}D(h_D - h_F)}{m_\Sigma - m_N} + \frac{\frac{17}{36}D(h_D + 3h_F)}{m_\Lambda - m_N} \\
&\quad + \frac{\left(\frac{17}{18}D^3 - \frac{19}{6}D^2F - \frac{13}{6}DF^2 + \frac{3}{2}F^3\right)h_D}{m_\Sigma - m_N} + \frac{\left(\frac{19}{18}D^3 + \frac{31}{6}D^2F + \frac{13}{6}DF^2 - \frac{3}{2}F^3\right)h_F}{m_\Sigma - m_N} \\
&\quad + \frac{\left(-\frac{37}{27}D^3 + \frac{11}{3}D^2F - \frac{4}{3}DF^2\right)h_D}{m_\Lambda - m_N} - \frac{\left(\frac{19}{9}D^3 - 5D^2F + 4DF^2\right)h_F}{m_\Lambda - m_N} \\
&\quad + \left(\frac{49}{27}D^3 - D^2F - \frac{19}{9}DF^2 + \frac{11}{3}F^3\right)\gamma_8, \\
\beta_{\Sigma^- n}^{(P)} &= \frac{\frac{17}{12}F(h_D - h_F)}{m_\Sigma - m_N} + \frac{\frac{17}{36}D(h_D + 3h_F)}{m_\Lambda - m_N} \\
&\quad + \frac{\left(\frac{10}{9}D^2F - 3DF^2 - F^3\right)h_D}{m_\Sigma - m_N} + \frac{\left(\frac{8}{9}D^2F + 5DF^2 + F^3\right)h_F}{m_\Sigma - m_N} \\
&\quad + \frac{\left(-\frac{37}{27}D^3 + \frac{11}{3}D^2F - \frac{4}{3}DF^2\right)h_D}{m_\Lambda - m_N} - \frac{\left(\frac{19}{9}D^3 - 5D^2F + 4DF^2\right)h_F}{m_\Lambda - m_N} \\
&\quad + \left(\frac{11}{18}D - \frac{11}{18}F + \frac{34}{27}D^3 + \frac{20}{9}D^2F - \frac{34}{9}DF^2\right)\gamma_8, \\
\beta_{\Lambda p}^{(P)} &= -\frac{\frac{17}{6}D(h_D - h_F)}{\sqrt{6}(m_\Sigma - m_N)} - \frac{\frac{17}{12}(D + F)(h_D + 3h_F)}{\sqrt{6}(m_\Lambda - m_N)} \\
&\quad + \frac{\left(-\frac{4}{9}D^3 + 6D^2F + 2DF^2\right)h_D}{\sqrt{6}(m_\Sigma - m_N)} - \frac{\left(\frac{32}{9}D^3 + 10D^2F + 2DF^2\right)h_F}{\sqrt{6}(m_\Sigma - m_N)} \\
&\quad + \frac{\left(\frac{61}{18}D^3 - \frac{137}{18}D^2F - \frac{35}{6}DF^2 + \frac{5}{2}F^3\right)h_D}{\sqrt{6}(m_\Lambda - m_N)} + \frac{\left(\frac{25}{6}D^3 - \frac{65}{6}D^2F + \frac{1}{2}DF^2 + \frac{15}{2}F^3\right)h_F}{\sqrt{6}(m_\Lambda - m_N)} \\
&\quad + \frac{1}{\sqrt{6}}\left(-\frac{11}{18}D - \frac{11}{6}F + D^3 + \frac{23}{9}D^2F + 3DF^2 + 5F^3\right)\gamma_8,
\end{aligned}$$

$$\begin{aligned}
\beta_{\Xi^-\Lambda}^{(P)} = & \frac{\frac{17}{6}D(h_D + h_F)}{\sqrt{6}(m_\Xi - m_\Sigma)} + \frac{\frac{17}{12}(D - F)(h_D - 3h_F)}{\sqrt{6}(m_\Xi - m_\Lambda)} \\
& + \frac{\left(\frac{4}{9}D^3 + 6D^2F - 2DF^2\right)h_D}{\sqrt{6}(m_\Xi - m_\Sigma)} - \frac{\left(\frac{32}{9}D^3 - 10D^2F + 2DF^2\right)h_F}{\sqrt{6}(m_\Xi - m_\Sigma)} \\
& - \frac{\left(\frac{61}{18}D^3 + \frac{137}{18}D^2F - \frac{35}{6}DF^2 - \frac{5}{2}F^3\right)h_D}{\sqrt{6}(m_\Xi - m_\Lambda)} + \frac{\left(\frac{25}{6}D^3 + \frac{65}{6}D^2F + \frac{1}{2}DF^2 - \frac{15}{2}F^3\right)h_F}{\sqrt{6}(m_\Xi - m_\Lambda)} \\
& + \frac{1}{\sqrt{6}}\left(-\frac{11}{18}D + \frac{11}{6}F + D^3 - \frac{23}{9}D^2F + 3DF^2 - 5F^3\right)\gamma_8.
\end{aligned}$$

From one-loop diagrams involving decuplet baryons, also shown in Figures 2 and 3,

$$\begin{aligned}
\beta_{\Sigma^+n}^{(S)} &= \frac{1}{2}\mathcal{C}^2(m_\Sigma - m_N)\gamma_8, \\
\beta_{\Sigma^-n}^{(S)} &= -\frac{1}{9}\mathcal{C}^2h_C + \mathcal{C}^2\left[-\frac{23}{18}(m_\Sigma - m_N) + \frac{8}{3}(m_\Delta - m_N) + \frac{13}{9}(m_{\Sigma^*} - m_N)\right]\gamma_8, \\
\beta_{\Lambda p}^{(S)} &= -\frac{1}{\sqrt{6}}\mathcal{C}^2h_C + \frac{1}{\sqrt{6}}\mathcal{C}^2\left[-(m_\Lambda - m_N) + 3(m_{\Sigma^*} - m_N)\right]\gamma_8, \\
\beta_{\Xi^-\Lambda}^{(S)} &= \frac{1}{\sqrt{6}}\mathcal{C}^2h_C + \frac{1}{\sqrt{6}}\mathcal{C}^2\left[\frac{4}{3}(m_\Xi - m_\Lambda) - 3(m_{\Sigma^*} - m_\Lambda) - \frac{16}{3}(m_{\Xi^*} - m_\Lambda)\right]\gamma_8, \\
\beta_{\Sigma^+n}^{(P)} &= \frac{-\frac{1}{9}D\mathcal{C}^2h_C + \left(-\frac{55}{162}\mathcal{H} + \frac{8}{27}D - \frac{4}{9}F\right)\mathcal{C}^2(h_D - h_F)}{m_\Sigma - m_N} \\
&+ \frac{\frac{1}{3}D\mathcal{C}^2h_C + \left(\frac{5}{162}\mathcal{H} - \frac{4}{9}D - \frac{4}{9}F\right)\mathcal{C}^2(h_D + 3h_F)}{m_\Lambda - m_N} + \left(-\frac{230}{243}\mathcal{H} + \frac{304}{81}D + \frac{16}{9}F\right)\mathcal{C}^2\gamma_8, \\
\beta_{\Sigma^-n}^{(P)} &= \frac{-\frac{1}{9}F\mathcal{C}^2h_C + \left(\frac{25}{54}\mathcal{H} - \frac{26}{27}D + \frac{2}{9}F\right)\mathcal{C}^2(h_D - h_F)}{m_\Sigma - m_N} \\
&+ \frac{\frac{1}{3}D\mathcal{C}^2h_C + \left(\frac{5}{162}\mathcal{H} - \frac{4}{9}D - \frac{4}{9}F\right)\mathcal{C}^2(h_D + 3h_F)}{m_\Lambda - m_N} + \left(\frac{170}{243}\mathcal{H} + \frac{82}{81}D + \frac{22}{27}F\right)\mathcal{C}^2\gamma_8, \\
\beta_{\Lambda p}^{(P)} &= \frac{\frac{2}{9}D\mathcal{C}^2h_C + \left(-\frac{5}{27}\mathcal{H} + \frac{8}{3}D + \frac{8}{3}F\right)\mathcal{C}^2(h_D - h_F)}{\sqrt{6}(m_\Sigma - m_N)} \\
&- \frac{(D + F)\mathcal{C}^2h_C + \left(\frac{10}{81}\mathcal{H} - \frac{2}{3}D - \frac{2}{9}F\right)\mathcal{C}^2(h_D + 3h_F)}{\sqrt{6}(m_\Lambda - m_N)} + \frac{1}{\sqrt{6}}\left(-\frac{20}{27}\mathcal{H} + \frac{106}{27}D + 6F\right)\mathcal{C}^2\gamma_8, \\
\beta_{\Xi^-\Lambda}^{(P)} &= \frac{\frac{22}{9}D\mathcal{C}^2h_C + \left(\frac{5}{27}\mathcal{H} - \frac{8}{3}D - \frac{8}{3}F\right)\mathcal{C}^2(h_D + h_F)}{\sqrt{6}(m_\Xi - m_\Sigma)} \\
&- \frac{(D - F)\mathcal{C}^2h_C + \left(\frac{20}{81}\mathcal{H} + \frac{14}{27}D + 2F\right)\mathcal{C}^2(h_D - 3h_F)}{\sqrt{6}(m_\Xi - m_\Lambda)} - \frac{1}{\sqrt{6}}\left(\frac{80}{81}\mathcal{H} + \frac{58}{27}D + \frac{58}{9}F\right)\mathcal{C}^2\gamma_8.
\end{aligned}$$

The contributions from the wave-function renormalization of the pion and the octet baryons and from the renormalization of the pion-decay constant are collected into

$$\bar{\lambda}_{BB'\pi} = \frac{1}{2}(\bar{\lambda}_B + \bar{\lambda}_{B'} + \lambda_\pi) - \lambda_f ,$$

where $\bar{\lambda}_B = \lambda_B + \lambda'_B$, λ_π and λ_f are defined by

$$\left(Z_B, Z_\pi, \frac{f_\pi}{f} \right) = 1 + (\bar{\lambda}_B, \lambda_\pi, \lambda_f) \frac{m_K^2}{16\pi^2 f_P^2} \ln \frac{m_K^2}{\mu^2} ,$$

with

$$\begin{aligned} \lambda_N &= \frac{17}{6}D^2 - 5DF + \frac{15}{2}F^2 , & \lambda'_N &= \frac{1}{2}\mathcal{C}^2 , \\ \lambda_\Lambda &= \frac{7}{3}D^2 + 9F^2 , & \lambda'_\Lambda &= \mathcal{C}^2 , \\ \lambda_\Sigma &= \frac{13}{3}D^2 + 3F^2 , & \lambda'_\Sigma &= \frac{7}{3}\mathcal{C}^2 , \\ \lambda_\Xi &= \frac{17}{6}D^2 + 5DF + \frac{15}{2}F^2 , & \lambda'_\Xi &= \frac{13}{6}\mathcal{C}^2 , \\ \lambda_\pi &= -\frac{1}{3} , & \lambda_f &= -\frac{1}{2} . \end{aligned}$$

One-loop corrections to the propagator that appears in tree-level pole diagrams in the P-waves yield the term $\tilde{\alpha}_{BB'}^{(P)}$. Its expression is equal to that of $\alpha_{BB'}^{(P)}$ with the exception that each factor $1/(m_X - m_Y)$ in $\alpha_{BB'}^{(P)}$ is replaced with $\mu_{XY}/(m_X - m_Y)$, where

$$\mu_{XY} = -(\bar{\beta}_X - \bar{\beta}_Y) \frac{m_K^3}{16\pi f_P^2} + [(\bar{\gamma}_X - \bar{\gamma}_Y - \bar{\lambda}_X \alpha_X + \bar{\lambda}_Y \alpha_Y) m_s + (\lambda'_X - \lambda'_Y) \Delta m] \frac{m_K^2}{16\pi^2 f_P^2} \ln \frac{m_K^2}{\mu^2} ,$$

with

$$\alpha_N = -2(b_D - b_F) - 2\sigma , \quad \alpha_\Lambda = -\frac{8}{3}b_D - 2\sigma , \quad \alpha_\Sigma = -2\sigma , \quad \alpha_\Xi = -2(b_D + b_F) - 2\sigma ,$$

$$\begin{aligned} \bar{\beta}_N &= \frac{5}{3}D^2 - 2DF + 3F^2 + \frac{4}{9\sqrt{3}}(D^2 - 6DF + 9F^2) + \frac{1}{3}\mathcal{C}^2 , \\ \bar{\beta}_\Lambda &= \frac{2}{3}D^2 + 6F^2 + \frac{16}{9\sqrt{3}}D^2 + \frac{2}{3}\mathcal{C}^2 , \\ \bar{\beta}_\Sigma &= 2D^2 + 2F^2 + \frac{16}{9\sqrt{3}}D^2 + \left(\frac{10}{9} + \frac{8}{9\sqrt{3}}\right)\mathcal{C}^2 , \\ \bar{\beta}_\Xi &= \frac{5}{3}D^2 + 2DF + 3F^2 + \frac{4}{9\sqrt{3}}(D^2 + 6DF + 9F^2) + \left(1 + \frac{8}{9\sqrt{3}}\right)\mathcal{C}^2 , \end{aligned}$$

$$\begin{aligned} \bar{\gamma}_N &= \frac{43}{9}b_D - \frac{25}{9}b_F - b_D \left(\frac{4}{3}D^2 + 12F^2\right) + b_F \left(\frac{2}{3}D^2 - 4DF + 6F^2\right) + \frac{52}{9}\sigma - 2\sigma\lambda_N \\ &\quad + \frac{1}{3}c\mathcal{C}^2 - 2\tilde{\sigma}\lambda'_N , \end{aligned}$$

$$\bar{\gamma}_\Lambda = \frac{154}{27}b_D - b_D \left(\frac{50}{9}D^2 + 18F^2\right) + b_F (12DF) + \frac{52}{9}\sigma - 2\sigma\lambda_\Lambda + \frac{4}{3}c\mathcal{C}^2 - 2\tilde{\sigma}\lambda'_\Lambda ,$$

$$\bar{\gamma}_\Sigma = 2b_D - b_D (6D^2 + 6F^2) - b_F (12DF) + \frac{52}{9}\sigma - 2\sigma\lambda_\Sigma + \frac{8}{9}c\mathcal{C}^2 - 2\tilde{\sigma}\lambda'_\Sigma ,$$

$$\begin{aligned} \bar{\gamma}_\Xi &= \frac{43}{9}b_D + \frac{25}{9}b_F - b_D \left(\frac{4}{3}D^2 + 12F^2\right) - b_F \left(\frac{2}{3}D^2 + 4DF + 6F^2\right) + \frac{52}{9}\sigma - 2\sigma\lambda_\Xi \\ &\quad + \frac{29}{9}c\mathcal{C}^2 - 2\tilde{\sigma}\lambda'_\Xi . \end{aligned}$$

References

- [1] J. Bijnens, H. Sonoda and M. B. Wise, Nucl. Phys. B **261**, 185 (1985).
- [2] E. Jenkins, Nucl. Phys. B **375**, 561 (1992).
- [3] E. Jenkins and A. Manohar, in *Effective Field Theories of the Standard Model*, edited by U.-G. Meissner (World Scientific, Singapore, 1992).
- [4] C. Carone and H. Georgi, Nucl. Phys. B **375**, 243 (1992).
- [5] R. P. Springer, hep-ph/9508324.
- [6] B. Borasoy and B. R. Holstein, Eur. Phys. J. C **6**, 85 (1999).
- [7] X.-G. He and G. Valencia, Phys. Lett. B **409**, 469 (1997); **418**, 443 (E) (1998).
- [8] A. Abd El-Hady, J. Tandean and G. Valencia, Nucl. Phys. A **651**, 71 (1999).
- [9] H. Georgi, *Weak Interactions and Modern Particle Theory* (The Benjamin/Cummings Publishing Company, Menlo Park, 1984); J. F. Donoghue, E. Golowich and B. R. Holstein, *Dynamics of the Standard Model* (Cambridge University Press, Cambridge, 1992).
- [10] E. Jenkins and A. V. Manohar, Phys. Lett. B **255**, 558 (1991).
- [11] E. Jenkins and A. Manohar, Phys. Lett. B **259**, 353 (1991).
- [12] E. Jenkins, Nucl. Phys. B **368**, 190 (1992).
- [13] O. E. Ovanesyan, in Review of Particle Properties, Phys. Lett. **111B**, 286 (1982).
- [14] U.-G. Meissner, hep-ph/9711365.
- [15] Review of Particle Physics. C. Caso *et. al.*, Eur. Phys. J. C **3**, 1 (1998).
- [16] B. W. Lee, Phys. Rev. Lett. **12**, 83 (1964); H. Sugawara, Prog. Theor. Phys. **31**, 213 (1964).
- [17] See, e.g., V. Bernard, N. Kaiser, and U.-G. Meissner, Z. Phys. C **60**, 111 (1993); B. Borasoy and U.-G. Meissner, Phys. Lett B **365**, 285 (1996); Ann. Phys. (N.Y.) **254**, 192 (1997); L. Durand and P. Ha, Phys. Rev. D **58**, 013010 (1998).
- [18] A. Manohar and H. Georgi, Nucl. Phys. B **234**, 189 (1984). H. Georgi and L. Randall, Nucl. Phys. B **276**, 241 (1986).
- [19] E. Jenkins *et al.*, Phys. Lett. B **302**, 482 (1993).
- [20] M. Butler, M. Savage, and R. Springer, Nucl. Phys. B **399**, 69 (1993).